
**Liquid Crystals**
Publication details, including instructions for authors and subscription information:
http://www.informaworld.com/smpp/title~content=t713926090

# Rayleigh scattering of a new lyotropic nematic liquid crystal system: crossover of propagative and diffusive behaviour

M. B. Lacerda Santos[a]; E. A. Oliveira[b]; A. M. Figueiredo Neto[b]
[a] Instituto de Física, Universidade de Brasília, 70910-900 Brasília, DF, Brazil, [b] Instituto de Física, Universidade de São Paulo, Cx.P. 66318, 05315-970 São Paulo, SP, Brazil,

Online publication date: 06 August 2010

**To cite this Article** Santos, M. B. Lacerda , Oliveira, E. A. and Neto, A. M. Figueiredo(2000) 'Rayleigh scattering of a new lyotropic nematic liquid crystal system: crossover of propagative and diffusive behaviour', Liquid Crystals, 27: 11, 1485 — 1495
**To link to this Article: DOI:** 10.1080/026782900750018654
**URL:** http://dx.doi.org/10.1080/026782900750018654

LIQUID CRYSTALS, 2000, VOL. 27, NO. 11, 1485–1495

# Rayleigh scattering of a new lyotropic nematic liquid crystal system: crossover of propagative and diffusive behaviour

M. B. LACERDA SANTOS*
Instituto de Física, Universidade de Brasília, 70910-900 Brasília, DF, Brazil

E. A. OLIVEIRA and A. M. FIGUEIREDO NETO
Instituto de Física, Universidade de São Paulo, Cx.P. 66318, 05315-970
São Paulo, SP, Brazil

(*Received 17 December 1999; in final form 3 April 2000; accepted 18 May 2000*)

In this paper we present to our knowledge the first light-scattering measurements on a rather new lyotropic system potassium laurate, decylammonium chloride, $H_2O$. Relative concentrations were chosen in order to obtain the discotic $N_D$ phase over a large temperature range. Measurements involve digital recording of the autocorrelation function resulting from self-beating of the depolarized scattered light. They were carried out at a fixed temperature in the $N_D$ phase range, by varying the scattering angle. A strong tendency to oscillations, superimposed on the usual relaxation signal, was found. This behaviour is quite surprising, as special precautions had been taken to minimize any eventual propagative signal. Such precautions have been tested previously, while investigating the older system potassium laurate, decanol, $D_2O$. Nevertheless, we have found that in the new lyotropic system, a propagative component may occur in a significant way, or even become dominant for some particular situations. Actually, the characterization of such situations is the main purpose of the present paper. Based upon a detailed analysis of photocorrelation data, it will be shown that the observed behaviour is consistent with the expected wave vector dependences of propagative and diffusive modes. Finally, a discussion is given on possible causes for the tendency to instability of lyotropic nematic liquid crystals.



## 1. Introduction

As is well known, the long range orientational order of nematic liquid crystals is subject to important thermal fluctuations which are responsible for a strong light scattering. The case of lyotropic nematics is particularly rich owing not only to additional phase transition phenomena [1] compared with thermotropic nematics, but also to the lability of their basic constituents [2, 3], which are aggregates of amphiphilic molecules, the so-called micelles. Furthermore, the presence of propagative components in the photocorrelation signal is a common occurrence that bears witness to the strong tendency of these systems to convective instability. Although often undesirable, such effects are interesting in themselves and have potential applications to be used, for instance, as a tool for studying the coupling between order and flow in liquid crystals.

In this paper we present, to our knowledge, the first Rayleigh light scattering measurements on a rather new lyotropic system—potassium laurate, decylamonium chloride, $H_2O$ (hereafter called LK-DaCl-$H_2O$). Relative concentrations were chosen [4] in order to obtain the discotic nematic $N_D$ phase over a large temperature range. All previous light-scattering investigations quoted here refer to the older lyotropic nematic system potassium laurate, decanol, $D_2O$ (hereafter called LK-D-$D_2O$) [5–7]. Although less known, the new system seems to behave qualitatively like the old one, according to a few structural studies [4, 8] presently available. For example, depending on the relative concentrations, both systems may present the three types of nematic phase known, namely two uniaxial ($N_D$ and $N_C$) and one biaxial ($N_B$).

The principle of the Rayleigh light scattering experiment can be summarized as follows. Let $\mathbf{n}_o$ be the unit vector specifying the average direction of alignment, that is, the optic axis. Following de Gennes [9], the fluctuations of the local director $\mathbf{n}$ may be expressed in terms of normal modes parallel and perpendicular to the plane defined by $\mathbf{n}_o$ and a given wave vector $\mathbf{q}$, according to $\mathbf{n} = \mathbf{n}_o + \delta n_1 \mathbf{e}_1 + \delta n_2 \mathbf{e}_2$. Here, the (parallel) mode $\delta n_1$ is made of a combination of splay and bend deformations, while the (perpendicular) mode $\delta n_2$ combines twist and bend. The director fluctuations have characteristic relaxation or damping rates, $\Gamma$, and for

*Author for correspondence; e-mail: marcus@fis.unb.br

*Liquid Crystals* ISSN 0267-8292 print/ISSN 1366-5855 online © 2000 Taylor & Francis Ltd
http://www.tandf.co.uk/journals

a long time [9] photon correlation techniques have been used to measure them. Such measurements yield information about elastic and viscous properties of the nematic system, as $\Gamma$ is given by

$$\Gamma_i = \frac{1}{\eta_i(\mathbf{q})}(K_i q_\perp^2 + K_3 q_\parallel^2) \qquad (1)$$

where $i = 1$, (2) labels the above-defined fluctuation modes, while $q_\parallel (q_\perp)$ is the component of the scattering wavevector $\mathbf{q}$ parallel (normal) to the optic axis. $K_1$, $K_2$ and $K_3$ are the Frank elastic constants characterizing, respectively, splay, twist and bend deformations.

Some particular scattering geometries may lead to a simpler $q$-dependence. For instance, for $\mathbf{q} \perp \mathbf{n}_o$ (see figure 1), pure deformations of twist can be probed for depolarized scattering, giving

$$\Gamma_{\text{twist}} = \frac{K_2}{\eta_{\text{twist}}} q^2 \equiv D_{\text{twist}} q^2 \qquad (2)$$

where $\eta_{\text{twist}} \equiv \gamma_1$ is the rotational viscosity coefficient [9]. This 'twist geometry' is indeed a suitable choice for working with the $N_D$ phase of our lyotropic system, considering its natural tendency to align the nematic director perpendicularly to the glass plates of the sample holder. All measurements reported here were taken in this geometry, at a fixed temperature in the $N_D$ phase range far from phase transitions. Basically, they consist of recording the autocorrelation function resulting from the self-beating of the depolarized scattered light. Different scattering angles were used, allowing us to measure the lifetime of Fourier components of twist fluctuations belonging to different wave vector moduli.



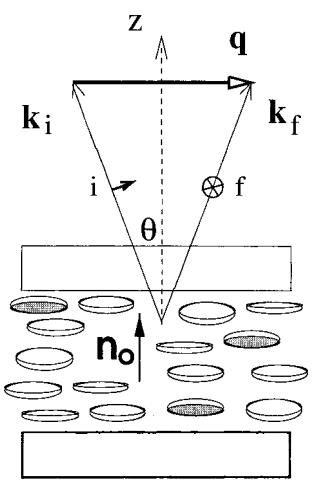


Figure 1. Schematics of the geometry used for depolarized scattering. The average director $\mathbf{n}_o$ of the fluctuating disk-like micelles points perpendicular to the glass plates ($z$-axis). This configuration with $\mathbf{q}$ perpendicular to $\mathbf{n}_o$ is suitable for measurements of damping rates of (expected) pure twist fluctuations of wave vector $\mathbf{q}$.

Usually, the most commonly observed autocorrelation functions in Rayleigh experiments with lyotropic nematics are the superposition of exponentially decaying functions. As we have seen above, director fluctuations are one possible explanation for them (but not the only one, as can be seen in [3]). In the measurements reported here, on the other hand, we have found a strong tendency to oscillations.

Oscillatory autocorrelation functions are commonly associated with flow. There is much literature exploring such phenomena, indeed a whole field of research, called laser Doppler anemometry. It is based on the principle [10] that light scattered by a volume element moving across with a velocity $\mathbf{v}$ suffers a frequency shift $\Delta\omega \equiv \omega - \omega_o$ proportional to the velocity component parallel to the scattering wavevector $\mathbf{q}$. In the case of Rayleigh scattering, we set $\omega_o = 0$ and write

$$\omega = \mathbf{q} \quad \mathbf{v}. \qquad (3)$$

Nevertheless, the presence of such oscillations here is quite surprising, for two reasons. Firstly, depolarized light is not expected to couple directly with flow. This objection however, is not so serious, for in the case of anisotropic fluids it is possible to formulate mechanisms allowing indirect coupling. The second reason, actually the important one, is that we have adopted special precautions to minimize any eventual propagative signal. Such precautions became standard in our light scattering experiments with lyotropic nematics a long time ago, while investigating the older system LK-D-$D_2O$. They consist basically of four points which are described in § 2.

In spite of such precautions, we have found that for some particular situations the propagative component may become very important, or even dominate the spectra. In other situations the oscillations may practically disappear, typically by changing the scattering angle. Although this single parameter does not allow a complete 'control' of such complex phenomena, we point out as a major achievement of the present work, the clarification of the role of the wave vector in this matter. Specifically, we want to emphasize two main objectives of the present research. First, to resolve and characterize both relaxational (either diffusive and non-diffusive) and propagative fluctuations in the new lyotropic system LK-DaCl-$H_2O$. Second, to show evidence that, contrary to appearances, this new system is not necessarily more unstable than the old one, the LK-D-$D_2O$ system. Both systems can easily become unstable. The main difference is that in the new system the dynamics of the two kinds of fluctuations, namely propagative and diffusive, tend to 'interfere' with each other or, more precisely, to share a common frequency range. Finally, a discussion is given on possible explanations for the strong tendency to instability of lyotropic nematic systems.

The paper is organized in three sections plus the Conclusion. The first section is this Introduction, which gives a brief description of the fundamentals of the light scattering experiment in nematics, including the properties allowing identification of diffusive and propagative behaviour. Next, § 2 describes the experimental methods. Then, § 3 starts to discuss methods for analysing the several sorts of multi-component autocorrelation functions appearing in the experiment. Final results are then presented, as well as a discussion about possible sources of instabilities. A summary of the main results is given in the Conclusion.

## 2. Experimental

Details for preparing the lyotropic system LK-DaCl-$H_2O$ used here are described in [4]. As said before, the relative concentrations of the lyotropic system were chosen to yield a region of the phase diagram dominated by the discotic nematic ($N_D$) phase over a large temperature range. They are, in weight %, 34.5% of potassium laurate, 4.2% of decylamonium chloride and 61.3% of $H_2O$. The mixture is sealed in a Pyrex tube, homogenized by vigorous shaking combined with centrifugation and then left at rest for several weeks.

Next, special directions followed in preparing the sample for light scattering, as well as details of the light-beating technique itself are essentially the same as those explained in previous publications [2, 3, 11], and will be only briefly described here.

Just before filling a light-scattering cell, the lyotropic mixture is submitted to further centrifugation for one hour at 4000 rpm to sediment dust. Care must then be taken to pipette the lyotropic phase only from the upper part of the tube. The liquid is then transferred into a Hellma cell made of two circular glass plates separated by a flat ring having a thickness of 1 mm and an internal diameter of 15 mm. The parts of the cell are then assembled with the help of a specially designed mounting system, which assures high compression of the plates. This system practically eliminates water loss problems, as verified in earlier work [12, 2]. All glass surfaces were previously thoroughly cleaned (with strong detergent) and rinsed in hot deionized distilled water.

Next, the cell is placed with its plates lying horizontally in an oven in thermal contact with a circulating heat bath, controlled so that the long term thermal stability (1 h) is better than 0.1°C. The sample temperature is monitored with a chromel–constantan thermocouple.

The low temperature limit of the $N_D$ phase recorded with the sample effectively for use was 6.5°C. No attempt to find the high temperature limit was made using the sample transferred to the scattering cell. However, in the Pyrex tube, the mixture remained in the $N_D$ phase up to a temperature as high as 55°C. Previous determination [4] of this $T_c$ for the same concentrations used here gave 75°C. All measurements in our light-scattering experiment have been taken at a fixed temperature of 31.7°C, far from phase transitions.

Turning to the sample alignment, untreated glass plates alone can impose good perpendicular orientation on the optical axis of the $N_D$ phase of our lyotropic system. However, considering the 1 mm thickness of our scattering cell, this so called homeotropic texture takes several days to set up in a sample left at rest. Fortunately, this waiting time can be reduced to a few hours with the help of a magnetic field. Note however that as the $N_D$ phase has a negative diamagnetic anisotropy, a magnetic field alone is not able to orient the nematic director in a homogeneous direction. However, using the combined effect of a magnetic field of about 5 kG parallel to the glass plates, plus the wall effects provided by them, we did succeed in obtaining well oriented samples with the optic axis perpendicular to the glass plates. This improved homeotropic texture is indeed very stable, and can survive without a magnetic field during several hours with a high degree of quality. We used this fact to perform the measurement runs without influence of the field.

In doing so, we monitored periodically the quality of the alignment. The method used was to check the uniformity (across a large area of the sample around the laser beam) of the colour observed when polarized white light traversed the sample at oblique incidence. This procedure, though quite simple, has been found previously [13] to be practically as good (for alignment verification) as a sophisticated method based on conoscopic images [14]. In fact, there is a simple reason for the high sensitivity of such polarized light observations, as it can be shown [15] that a small distortion $\theta$ in the homeotropic texture causes a change in the local light intensity $I$ according to $I/I_o \sim \theta^4$, where $I_o$ is the input intensity.

Figure 1 schematizes the scattering geometry. A 35 mW HeNe laser (Spectra Physics, mod. 127) beam oriented along $\mathbf{k}_i$ traverses the sample cell making an (internal) angle of $\theta/2$ with respect to the glass plate normal ($z$-axis). The selection of the scattered wave vector $\mathbf{k}_f$ direction follows an optical alignment procedure that makes use of the reflected beam from the cell, yielding a symmetrical geometry with respect to the $z$-axis which enables a precise definition of the scattering plane ($y, z$).

The incident polarization vector $\mathbf{i}_o$ is made parallel to the scattering plane by a Nicol prism regulated within better than 0.5°C. A polarizer sheet is used to define the polarization of the scattered beam either parallel or perpendicular to the scattering plane. The first (second) choice corresponds to the ordinary (extraordinary) polarization, specified by the unit vector $\mathbf{f}_o$ ($\mathbf{f}_e$). For any one

of the depolarized configurations [either (o,e) or (e,o)], the geometry of figure 1, with $\mathbf{q} \perp \mathbf{n}_o$, provides optical coupling with mode 2.

Notice that even for depolarized scattering we can take $|\mathbf{k}_i| \approx |\mathbf{k}_f|$, due to the low birefringence of lyotropic nematics [12] ($\Delta n \sim 10^{-3}$). Therefore, $\mathbf{q}$ is practically parallel to the $y$-axis. In consequence, mode 2 gives pure twist deformations, allowing us to expect that the fluctuations relax according to the simple formula in equation (2), as said in the Introduction.

In order to calculate $|\mathbf{k}|$ we used a (mean) refractive index $n = 1.38$, which was determined for the LK-D-$D_2O$ system [12]. The four values of $q$ used in the experiment are in units of $10^6\ m^{-1}$: $q_1 = 2.08$, $q_2 = 3.12$, $q_3 = 3.49$, and $q_4 = 4.44$.

Next, the selected scattered light beam is collected by a pinhole with opening area $A \ll A_c$, where $A_c$ is the coherence area [16], and then focused onto the photocathode of the photomultiplier tube (ITT, mod. FW-130). The whole optical set-up is assembled on a heavy bench floating on pneumatics to prevent mechanical vibrations. Detailed information about our light-beating spectrometer has been given elsewhere [17].

The output pulses of the photomultiplier are square shaped by a pre-amplifier discriminator (PAR 1182) and then sent to the photon correlator. A description of our software correlator has been published elsewhere [18]. Let us simply mention here that it uses 14 bit registers, which are more suitable to deal with slow signals (< 10 Hz) than the conventional 4 bit correlators. Indeed, such large registers prevent attenuation of the optical signal over long time scales, allowing more rapid accumulation of data.

We are now in position to list the four precautions that we took in the experiment in order to minimize propagative components in the signal. They are: (1) to maintain the horizontal positioning of the sample cell; (2) to avoid excessive laser power on the sample; (3) to wait a long time to ensure stabilization of the sample after any thermal or mechanical disturbance; (4) to keep the thermal isolation of the sample as good as possible. Adhering to this last point is limited in our light-scattering experiment in which one wishes to have optical access to the sample at several angles.

## 3. Results and discussion

### 3.1. *Methodology for data analysis*

We start this section by discussing how to analyse some illustrative examples of autocorrelation functions obtained in the experiment with the LK-DaCl-$H_2O$ system. As said in the Introduction, the striking feature about these curves is the presence of oscillatory components in most of them. This contrasts with the usual behaviour, as described in previous studies in the old LK-D-$D_2O$ system, where such propagative components were absent or, at least, could be kept at a negligible level. Consequently, some modification in the methods of analysis is required to deal with such data. At first sight, the whole task seems to reduce to a simple matter of choosing mathematical functions with the appropriate shape, that is, the fitting curves. However, one must realize that the information contained in spectral signals is limited by factors like noise, finite resolution and finite range. Then, care must be taken when selecting the fitting functions in order to avoid either stability problems or creation of too many artefacts. With this in mind, we adopt, as a rule, the following two procedures. First, we try to be conservative in the number of parameters. Second, before the number of parameters is increased, tests are made with forms demanding fewer parameters, even in a rough approximation, in order to keep as much control as possible of the process.

Three representative examples of autocorrelation functions obtained in the experiment are shown in figures 2 to 4. They will be useful to illustrate not only the occurrence of propagative components at different levels of strength, but also the variations in the mathematical modelling employed. Like all measurements reported here, they are depolarized signals obtained in the 'twist geometry' (figure 1).

Figure 2 shows a signal obtained for $q = q_3$ with a resolution time (or sample time) of $\Delta\tau = 200$ ms per channel. [The 128 channel (experimental) points are plotted as centred vertical bars, in this figure.] It represents a class of signals with excellent signal-to-noise ratio and showing a well defined oscillatory component. How can we model, mathematically speaking, such a photocorrelation curve? As a first proposal, let us try an exponential superimposed to a cosinus function, such as

$$y = A_1 \exp(-t/\tau) + A_2 \cos(2\pi t/T_o + \phi) + B \qquad (4)$$

with $A_1$, $A_2$, $\tau$, $T_o$, $\phi$ and $B$ as adjustable parameters. In the case of figure 2 the best values for these are $A_1 = 1.128 \times 10^7$, $\tau = 40.6$ s, $A_2 = 1.288 \times 10^5$, $T_o = 13.7$ s, $\phi = 5.63$ and $B = 7.11 \times 10^6$. The resulting curve fits the data pretty well, as we can see in the figure (continuous curve).

Of course, not all photocorrelation functions of the experiment have the quality shown by the signal of figure 2. In fact, many factors may intervene to cause a rather important dispersion in the quality of the signals. We will not enter into such technical matters here (overviewed in [3]). As we are concerned with characteristic times and not with intensities, what matters for us is the shape of the curve (besides the time scales). In this respect, it is interesting to note that the sum of an exponential plus a cosinus (exp + cosinus, for short) turned out to be the most successful fitting curve of the

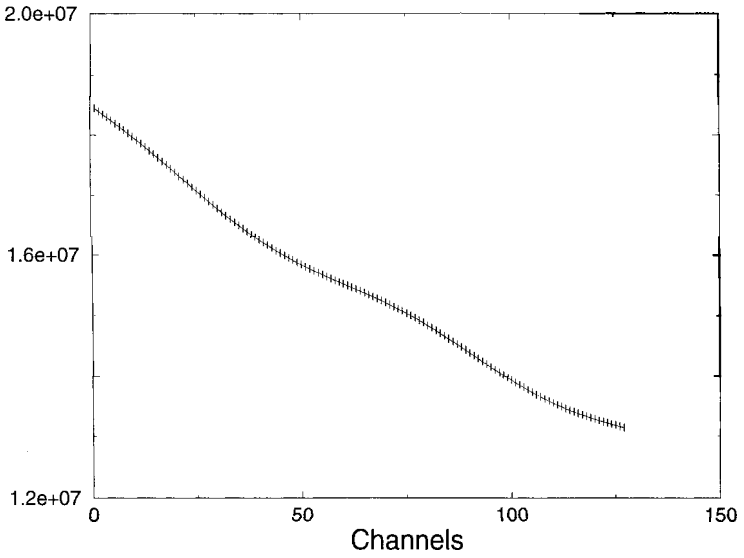


Figure 2. Example of a depolarized light signal carrying a strong propagative component superimposed on the usual twist relaxation. The autocorrelation function ('‖') was fitted with an exponential plus a cosinus function ('−'). Relevant parameters of this spectrum are as follows. Wave vector: $q_3 = 3.49 \times 10^6\ m^{-1}$; time scale: $\Delta\tau = 200$ ms per channel. See also the text.

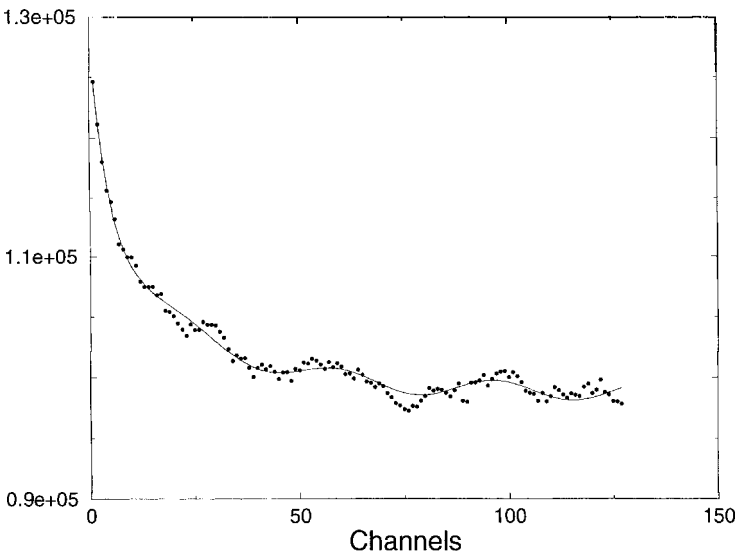


Figure 3. More complex than the preceding case (figure 2), this example requires two exponentials plus a cosinus function for an approximative fitting. Wave vector: $q_4 = 4.44 \times 10^6\ m^{-1}$; time scale: $\Delta\tau = 30$ ms. See also the text.

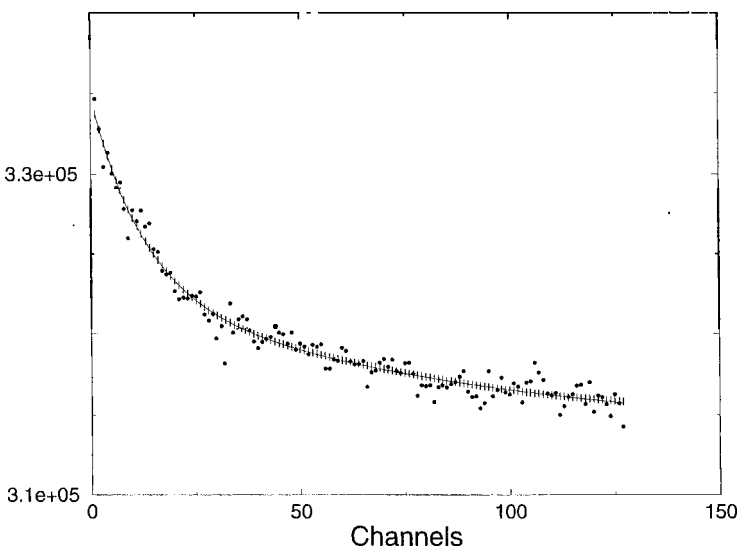


Figure 4. Propagative or diffusive situation? Example of a depolarized light signal carrying a weak long-time component. The two exponential ('−') and the exponential + cosinus ('‖') models fit equally well. Wave vector: $q_1 = 2.08 \times 10^6\ m^{-1}$; time scale: $\Delta\tau = 30$ ms. See also the text.

experiments. That is, after testing alternative forms, the exp + cosinus form was the most efficient in about 70% of the recorded spectra.

Now, let us look at the signal shown in figure 3. (Wave vector: $q = q_4$; time scale: $\Delta\tau = 30$ ms.) More complex than the preceding case, this example requires two exponentials to account for its relaxational dynamics only. By adding a cosinus term, we tried the least squares fit for this signal with the function

$$y = A_1 \exp(-t/\tau_1) + A_2 \exp(-t/\tau_2) + A_3 \cos(2\pi t/T_0 + \phi) + B \quad (5)$$

resulting in the following set of eight best parameters: $A_1 = 1.637 \times 10^4$, $\tau_1 = 0.122$ s, $A_2 = 1.416 \times 10^4$, $\tau_2 = 0.718$ s, $A_3 = 7.39 \times 10^2$, $T_o = 1.12$ s, $\phi = 2.56$ and $B = 9.876 \times 10^4$. We see that this 2-exp + cosinus form accounts well for the relaxation times, although it may appear poor for oscillations. However, a closer look suggests that a mode structure might be present. That is, our cosinus would have caught the fundamental 'note'.

The last example illustrates a rather degenerate situation. The signal of figure 4 was obtained for $q = q_1$ at a resolution time $\Delta\tau = 30$ ms. It represents a minority type of signal (15–20%) in the experiment for which the nature of the long-time component, whether it is oscillatory or exponentially decaying, it is not clear. So, our first attempt to treat such signals is to try both forms of fitting. Often, in these cases of weak long-time components, only the 2-exponential fit works. The reason is that 2-exp is a more stable function than exp + cosinus, as it is easy to check mathematically by calculating the error propagations in the corresponding expressions due to an error $\Delta\tau_2$, keeping all other parameters fixed. This results, in the 2-exp case (equation (5), with $A_3 = 0$),

$$|\Delta y| = A_2/\tau_2 \exp(-t/\tau_2)|\Delta\tau_2| \quad (6)$$

and, in the exp + cosinus case (equation (4), with $\tau_2$ replacing $T_o$),

$$|\Delta y| = 2\pi A_2/\tau_2 \sin(2\pi t/\tau_2 + \phi)|\Delta\tau_2|. \quad (7)$$

So, we can see that, as times goes on, the error due to the uncertainty $\Delta\tau_2$ decays exponentially for the 2-exponential fit, while in the case of the exp + cosinus fit, it remains oscillating forever.

Indeed, signals giving good 2-exponential fits are the ordinary situation in experiments with the old lyotropic system (LK-D-$D_2O$), though they are a minority of cases here. Turning back to the case illustrated by figure 4, in which both fits are satisfactory, the question is how to decide between the two forms?

In the example, the best parameters for 2-exp are (again, referring to equation (5), with $A_3 = 0$), $A_1 = 1.249 \times 10^4$, $\tau_1 = 0.39$ s, $A_2 = 9.300 \times 10^4$, $\tau_2 = 3.16$ s and $B = 3.130 \times 10^5$. On the other hand, the best parameters for exp + cosinus, equation (4), are: $A_1 = 1.514 \times 10^4$, $\tau = 0.45$ s, $A_2 = 1.91 \times 10^3$, $T_o = 8.63$ s and $B = 3.176 \times 10^5$. Thus, we note that the short-time is almost insensitive to the choice of the fit, but a significant discrepancy appears for the long-time component.

Looking at these figures, it is worth noting that the intensity of the long-time component is much stronger in the 2-exp fit than for the exp + cosinus. This could be understood if we admit the hypothesis that in the 2-exp fit the long-time component incorporates two contributions, the first one of a propagative nature (from hydrodynamic motions) and the second one from micellar fluctuations. Micellar fluctuations have been studied in the LK-D-$D_2O$ system [3, 2]. They are relaxational, but non-diffusive, i.e. $q$-independent. We shall return to micellar fluctuations in the next section. Here, the point is that the exp + cosinus fit would 'filter' the micellar contribution out, by taking an overall baseline at a (proportionally) higher level. Whenever this fit works, as in figure 4, it gives us the opportunity of keeping track of the propagative mode in such extreme situations in which it becomes less apparent. Moreover, the result is consistent with other data (see figure 5), and thus, in the context of the present paper, we prefer to choose the exp + cosinus fit in cases similar to that of figure 4. Now, we proceed to the systematic analysis of the complete set of data.

### 3.2. *Relaxation versus propagation*

Figures 5(*a*) and 5(*b*) show plots for relaxation (triangles and squares) and propagation (crosses and ×s) frequencies against the wave vector modulus $q$. All symbols refer to depolarized light and there are two different symbols to represent each class of phenomenon in order to keep track of the identity of two series of data. Both series were recorded with the same sample, at the same temperature (31.7°C) with five days of interval (triangles and ×s first) between each one. The data points for each one of the two series appear to have quite a degree of scatter. However, no systematic change can be distinguished between the two groups (which could be attributed, for instance, to a sample ageing effect). Thus, in this sense, we can say that the measurements are reproducible within the experimental error, and thus, hereafter, we can simply ignore the discrimination between the two series.

Another question is how to explain this 'experimental error' or even to quantify it. Indeed, the intriguing thing here is that such scattered data points come from good

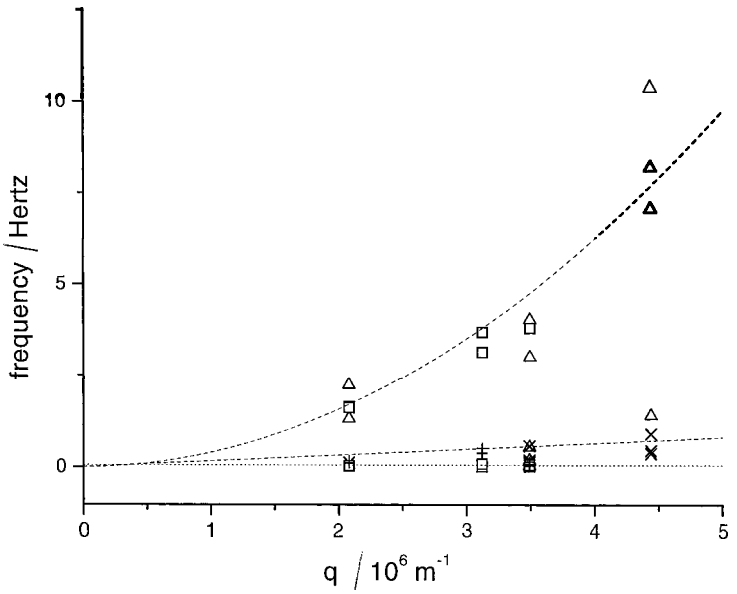


(*a*)

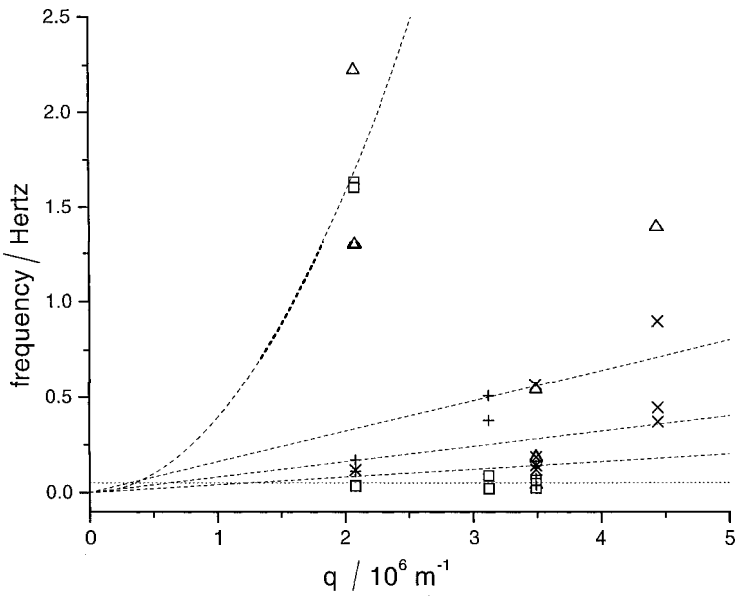


(*b*)

Figure 5. (*a*) Frequencies of fluctuations versus $q$. All symbols refer to depolarized light. Triangles and squares refer to two series of relaxation frequency data (damping rates), while symbols '+' and '×' refer as well to two such series of data, but for the oscillating frequencies from propagative contributions. (*b*) Scale amplification of the data of 5 (*a*) in order to resolve the lowest frequency data points, especially the propagative contributions. A multimode structure appears—see the text.



quality signals, like those shown in figures 2, 3 and 4. Thus, it is useless to mark in the plot the error bars associated with the autocorrelation data. Such errors are comparatively low, and cannot explain the scatter of the points of figures 5 (*a*) and 5 (*b*).

How, then, can it be that good quality correlation functions give such scattered data points? The reason for such behaviour remains basically an open question, as probably the full complexity of these fluctuations is not yet completely understood. Hypothetically, however, one could advance a kind of 'operational' explanation, by saying that the signals carry information on too many phenomena (orientational and micellar diffusion, plus propagative components), which makes the task of discriminating them virtually impossible with good precision.

Nevertheless, by looking at these frequency versus wave vector data for the LK-DaCl-$H_2O$ system, one can say that they split into two branches. The low frequency branch is formed by the propagative components,

while the higher branch comes from the relaxational components. By comparison with the better known LK-D-$D_2O$ system [11, 3, 2], the higher branch can be attributed to twist fluctuations. The diffusive behaviour of this component, predicted by equation (2), can help us to make the separation between the two branches more clear. In fact, in spite of the errors, the branch of relaxation data can be acceptably fitted to a parabola passing by the origin, according to equation (2). This yields the twist diffusivity coefficient, $D_{twist} = 0.39 \times 10^{-12}\,m^2\,s^{-1}$. Note that, in spite of depolarized scattering, the extrapolation to $q = 0$ is approximately true, because of the already mentioned low birefringence of lyotropic nematic liquid crystals.

Now let us consider the lowest frequency data arising from the long-time exponential component of the 2-exp or 2-exp + cosinus fit (triangles and squares). They are quite independent of $q$, although the $q_4$ data seems to be a little higher. A similar artefact has been noted before [3, 11], and was attributed to an 'attraction effect' of the high frequency of the twist signal at these high $q$ values. This interpretation should be revised now, after the discussion about the influence of the propagative mode in the fittings, at the end of § 3.1. In fact, the analysis of the 'degenerate case' of figure 4 showed that a contribution from the propagative mode may be present even when the oscillations are not apparent. Probably a more consistent explanation of the artefact mentioned is to suppose that this low relaxation frequency is indeed 'raised up', but preferentially by the propagative mode (as both contributions are mixed together in the 2-exp fit). Thus, by concentrating our attention on the lowest frequencies only (they are indicated on the plots by a horizontal dotted line at the level of 0.05 Hz) we recognize here, by its non-diffusive behaviour, the signature of the already studied micellar mode [3]. Ordinarily, micellar fluctuations are expected to give only polarized scattering. However, they appear systematically in our depolarized signals too, as a weak component compared with the full (o,o) signal. This component may be due to polarization leakage, but it is also possible to work out mechanisms for micellar fluctuations giving rise to depolarized scattering [3].

Finally, we now consider the propagative data, that is, the frequencies extracted from the oscillatory part of the autocorrelation functions (i.e. those fitted with forms like equations (4) and (5)). Such data appear in figures 5(*a*) and 5(*b*) as crosses and $\times$s. Although presenting a general tendency to increase smoothly as $q$ increases, the propagative frequencies cannot be fitted with a single linear relationship like equation (3). By amplifying the frequency scale, figure 5(*b*), however, a multimode structure might be seen, though rather spoiled by the experimental errors. As a guide to the eye, we have plotted three straight lines passing through the origin. Adopting a unit value for the lower slope, the other slopes are 2 and 4.

From the slope of the straight lines representing propagative modes we can deduce (noting that we have plotted the inverse of the periods, $T_o^{-1}$) that typical velocities in the hydrodynamic rolls ranges between 0.2 and 1.2 $\mu m\,s^{-1}$. These values are about the same as those obtained for the LK-D-$D_2O$ system [13] (actually, the upper limit here is a little higher than there), although the observation of convective phenomena in that system followed fairly different experimental conditions, as will be recalled in § 3.3.

Finally, an interesting connection can be made between these typical flow velocity values shared by the new and the old lyotropic systems, and the twist diffusivity coefficient found above. Recalling the published value for this same coefficient in the $N_D$ phase of the LK-D-$D_2O$ system [12], namely $D_{twist} = 1.6 \times 10^{-12}\,m^2\,s^{-1}$, we note that this value is about four times that just found for the LK-DaCl-$H_2O$ system. Therefore, we can talk of a crossover between the propagative and the diffusive modes as being the reason why the oscillations are so unavoidable in the case of the LK-DaCl-$H_2O$ system. These two kinds of mode simply become too close to each other in their time scales. This can be clearly seen in the figure 5(*a*). On the other hand, according to the quoted data, a parabola representing the twist relaxation in the old LK-D-$D_2O$ system would be much steeper, while any typical straight line representing a propagative mode would have a slope comparable to those appearing here for the new system.

### 3.3. *Why does it roll?*

The analysis of the data summarized in figure 5, shows evidence of convective motions present in the sample, in spite of the care taken to avoid them. It is obvious that there is a strong tendency to instability caused by some spurious, uncontrolled agent. As we are going to recall soon, such a tendency to instability is indeed also present in the old lyotropic system. The reason that it becomes more 'visible' with the new system has already been explained above.

An entirely different issue is to identify the agent causing such instabilities. This is an open question, which cannot be definitely answered by the present work. Thus, in what follows, we limit ourselves to discussing a few hypothetical mechanisms which could be at the basis of the observed propagative phenomena, and we try to evaluate the plausibility of each one.

#### 3.3.1. *Thermal convection*

Perhaps the first idea that arises when considering convective motions in a liquid is Bénard instability [19].

Although such a process requires a vertical temperature gradient above a certain threshold $\Delta T_c$ in order to take place, it is well known [20] that this threshold is much lower for a nematic liquid crystal. Dubois-Violette *et al.* [20] treated the problem of rod-like (or calamitic) nematic films heated from below and from above, considering two kinds of material according to the sign of their thermal conductivity anisotropy, $k_a = k_\parallel - k_\perp$, as either positive or negative. In order to extend their argument (heat focusing mechanism) to a nematic system made of disk-like objects, the key step is to recognize that in such systems velocity gradients normal to the equilibrium director $\mathbf{n}_o$ are the most effective to define the viscous torques. This is in contrast to the situation for rod-like nematics, in which velocity gradients parallel to $\mathbf{n}_o$ are the most effective in this way. This so called backflow problem is treated in detail in [11, 12] for lyotropic nematic liquid crystals.

With this in mind, it is not difficult to recycle the Dubois-Violette argument for our system and geometry, looking for the effect caused by a splay fluctuation in the presence of a vertical temperature gradient along the sample thickness $d$. As heat conduction data are not available for our system, let us assume that it behaves as normally expected for disks, that is, with negative $k_a$. We then find that our discotic nematic sample, initially homeotropic, should be unstable above $\Delta T_c$. The situation is analogous to that of a rod-like nematic sample with positive $k_a$, initially planar, analysed in [20] (see figure 1(*a*) therein). Both cases refer to heating from below. (Heating from above is stabilizing in our case.)

Thanks to the anisotropic mechanism, theory predicts for nematics a reduction of $\Delta T_c$ by a factor of the order of $10^3$ compared with the usual threshold for an ordinary liquid, given by [20] $Ra_c \approx 1708$, where the dimensionless Rayleigh number is defined as

$$Ra = \frac{\Delta T d^3 \rho g \alpha}{\kappa \eta}. \tag{8}$$

Here, $\rho$ is the density, $g$ is the acceleration due to gravity, $\alpha$ is the thermal expansion coefficient, $\kappa$ is the heat diffusivity, $\kappa = k/\rho C$ ($C$ = specific heat) and $\eta$ is the shear viscosity. We do not know figures for all these parameters for our system. In the case of MBBA, a classical nematic, it gives [20] for a sample with thickness $d = 1$ mm, $\Delta T_c \approx 2 \times 10^3$ °C, which becomes $\sim 2$°C, after applying the reduction factor. As an alternative estimate, if we put in the formula data for water (since our system is mainly made of water), and apply the factor, we get a threshold which is about the double the value estimated for MBBA.

Therefore, in spite of the dramatic reduction of the threshold for thermal convection in nematics, owing to the anisotropic mechanism, the estimates above indicate that $\Delta T_c$ is probably still too high to arise in a spurious way. Indeed, we have checked experimentally (using thermocouples attached to the top and bottom plates of our sample holder) that the (spurious) vertical gradient in the conditions of our light scattering experiment is always below 0.1°C mm$^{-1}$.

Finally, another test was done in connection with the *horizontal* temperature gradient, which could also be a source of instabilities. To this purpose, two thermocouples were attached 1 cm apart on the bottom glass plate of the sample holder. The measured residual temperature difference, under the conditions of the light scattering experiment, was less than 0.05°C, which means a gradient of 0.005°C mm$^{-1}$. Thermal convections induced by horizontal gradients are specially 'dangerous', as they need virtually no threshold [19] (they only need to overcome viscosity). However, considering the persistence of the propagative signal (accumulated during about 20 min), in contrast to the intermittence of this residual gradient, we find that such a mechanism can be ruled out here.

Let us also mention the mechanism of surface tension instability [19]. This is a free surface effect, so one could speculate about its possibility associated with a small air bubble always present in the sample cell. However, as this mechanism is also ultimately induced by temperature gradients, it can be ruled out as before.

Now, we recall a test made in an early study by one of us [13] concerning propagative effects in the old lyotropic system. Using a sample cell similar to the present one, but filled with the $N_D$ phase of the LK-D-$D_2O$ system, it was observed that simply standing the sample cell up (i.e. with its glass plates parallel to the vertical) dramatically reinforced the convective instability. No magnetic field was used in that test. Although the cause of the onset of the instability in that instance remains unknown, it is possible that in such a configuration the sample suffers a slight (spurious) horizontal temperature gradient. The phenomenon was strong enough to be visualized and photographed, by using polarized light (figure 25 of [13]). Rayleigh scattering measurements were then performed, by varying the magnitude of the scattering wave vector $\mathbf{q}$, while keeping its direction parallel to the vertical direction. This allowed verification of the relationship equation (3), yielding flow velocities ranging from 0.1 to 0.5 μm s$^{-1}$. Therefore, the flow velocities obtained in that test were in the same range as those obtained in the present work for the new lyotropic system.

### 3.3.2. *Demixing, flocculation*

Here is an instability mechanism controlled by a different 'driving force'. A concentration gradient can

generate convective rolls, called the Rayleigh–Taylor instability (for a recent study, see [21]). Indeed, samples in early experiments made by one of us [12, 2] had short lifetimes of a few weeks due to water losses by evaporation through the joints of the scattering cell. Thus, concentration gradients could be observed to occur as an ageing effect. However, this problem of water loss has been practically eliminated in our more recent experiments, and since then [3] our light scattering samples stay operational for years. Of course, in such long runs there may occur important drifts in transition temperatures (probably caused by residual water loss—typically of 1%/year—as witnessed by the increase in size of the air bubble), but no visible demixing has been observed in samples with a normal history. So, this mechanism should be discarded as explaining the presently observed propagative signal.

3.3.3. *Nematic relaxation in zero field*

Here we have a more serious source of perturbation. As explained in the Experimental section, a magnetic field (5 kG) is applied in order to improve the sample alignment. It is then removed a few hours before we start the light scattering measurements. The simple fact that the sample texture degrades after a delay of many hours is indicative that a slow process is occurring. Indeed, a characteristic time $\tau$ for such a nematic relaxation in zero field can be estimated using the formula (see [9], chap. 5) $\tau = \gamma_1 d^2/\pi^2 K_2$. Taking (in cgs units) $K_2 \sim 10^{-7}$ dy, $d = 10^{-1}$ cm and $\gamma_1 \sim 1$ P [12], we get $\tau \sim 3$ h.

During the experiments, the magnetic field was applied before each of the two series of data referred to above, and then withdrawn when the alignment was judged to be good. Let us call this time $t = 0$, for each of the series. The first series started at $t = 6$ h and finished at about $t = 12$ h. The second series started at $t = 2.5$ h and finished at $t = 9$ h. Looking at the figure estimated for $\tau$, one could say that a certain risk was taken at the beginning of the second series. Let us note, however, that this is only an order of magnitude estimate and, what is perhaps more important, that too much relaxation would after all mean poor alignment.

As a matter of fact, the second series started by giving a signal having a strong propagative component, which is, in fact, the signal shown in figure 2. However, we have recorded other signals having similar characteristics four, six and even ten hours after the removal of the magnetic field.

To conclude, among the several possibilities previously discussed, the mechanism of slow relaxation following removal of the magnetic field seems to be the most plausible explanation for the propagative effects observed in the conditions of the present experiment. If this is the case, however, it is something hard to avoid, at least if we want to work with well aligned samples. Of course, the same situation should affect the old lyotropic system too. Again, the above-described crossover effect makes the instabilities 'more bothering' in the present case than in the old one.

## 4. Conclusion

We have presented here results of our dynamical light scattering measurements on the new lyotropic system, KL-DaCl-$H_2O$. The striking feature of these measurements is that the autocorrelation functions show important oscillatory components. These oscillations are superimposed on the usual exponential decaying components, mainly due to director fluctuations.

A discussion of these results is made by comparison with analogous data obtained by one of us for the old lyotropic system KL-Decanol-$D_2O$. It is recalled that this old system also presented propagative components, which could even be very strong, under special conditions (described in [13] and briefly reviewed here). However, provided that such conditions were avoided, almost pure exponential autocorrelation functions were obtained, and thus, the propagative phenomena in the KL-Decanol-$D_2O$ system could remain as a 'laboratory curiosity'.

Now turning to the new system, based on a detailed analysis of the data, we have been able to show that the different forms of autocorrelation function produced by the experiment can be resolved into components having wave vector dependences of propagative and diffusive modes (besides a small, $q$-independent, long-time component).

So, we are led to the conclusion that, despite the appearances, the new system is *not* 'more unstable' than the old one. Both can show strong propagative components, if the conditions for this are fulfilled (e.g. to look for them in the appropriate time scales). Such conditions may be, in fact, quite subtle, often being provided in a spurious way. Therefore, why does the new system *seem* to be more unstable? Based on the analysis made here, this question can now be partially answered. It turns out that in the case of the KL-DaCl-$H_2O$ system, the propagative mode is 'situated' quite close to the diffusive one, as can be seen in figure 5 (*a*). Thus, the 'crossover', happens so to speak, which is much less noticeable in the old system, which has a twist diffusivity coefficient much larger than the new system.

Of course, there remains the question as to why there is such a relative proximity of the diffusive and propagative modes in the KL-DaCl-$H_2O$ system. Although this question is outwith the scope of the present investigation, let us mention that comparisons of structural data of the old [7] and the new [4] lyotropic systems suggest that the micelles in the new system are smaller and have

less anisometry. It would be interesting to carry out a theoretical study concerning the influence of these two factors on the dynamical behaviour of the fluctuations.

Finally, we have given a discussion of the possible agents that may be responsible for the general strong tendency to instability of lyotropic nematic liquid crystals. This too remains an open question, and will require more investigations on these systems (probably involving combined techniques and monitoring the history of the samples) to be satisfactorily answered.

It is a pleasure to thank G. Cajati and O. Portilho for valuable computational help as well as M. A. Amato for a critical reading of the manuscript. We also thank the referee for useful criticisms. Finally, A.M.F.N. wishes to thank CNPq, FAPESP and PRONEX for partial financial support.

## References

[1] Lacerda Santos, M. B., Galerne, Y., and Durand, G., 1984, *Phys. Rev. Lett.*, **53,** 787.
[2] Lacerda Santos, M. B., and Durand, G., 1986, *J. Phys. (Paris)*, **47,** 529.
[3] Lacerda Santos, M. B., Ferreira, W. B., and Amato, M. A., 1994, *Liq. Cryst.*, **16,** 287.
[4] Oliveira, E. A., Lièbert, L., and Figueiredo Neto, A. M., 1989, *Liq. Cryst.*, **5,** 1669.
[5] Yu, L. J., and Saupe, A., 1980, *Phys. Rev. Lett.*, **45,** 1000.
[6] Hendrikx, Y., Charvolin, J., Rawiso, M., Lièbert, L., and Holmes, M. C., 1983, *J. phys. Chem.*, **87,** 3991.
[7] Galerne, Y., Figueiredo Neto, A. M., and Lièbert, L., 1987, *J. chem. Phys.*, **87,** 1851.
[8] Bartolino, R., Chidichimo, G., Golemme, A., and Nicoletta, F. P., 1992, in *Phase Transitions in Liquid Crystals*, edited by S. Martelucci and A. N. Chester, NATO ASI Series, (New York: Plenum), pp. 427–438.
[9] de Gennes, P. G., 1974, *The Physics of Liquid Crystals* (Oxford: Clarendon Press).
[10] Tanaka, T., and Benedek, G. B., 1975, *Appl. Opt.*, **14,** 189.
[11] Lacerda Santos, M. B., and Amato, M. A., 1999, *Eur. Phys. J*, **B7,** 393.
[12] Lacerda Santos, M. B., Galerne, Y., and Durand, G., 1985, *J. Phys. (Paris)*, **46,** 933.
[13] Lacerda Santos, M. B., 1985, PhD. thesis, Orsay, France.
[14] Galerne, Y., and Marcerou, J. P., 1983, *Phys. Rev. Lett.*, **51,** 2109.
[15] Lacerda Santos, M. B., Licinio, P., and Durand, G., 1985, *Mol. Cryst. liq. Cryst. Lett.*, **2,** 15.
[16] Berne, B. J., and Pecora, R., 1976, *Dynamic Light Scattering* (New York: Wiley).
[17] Lacerda Santos, M. B., 1992, *Rev. Fis. Aplic. Instr.*, **7,** 1 (in Portuguese).
[18] Jota, F. G., Braga, A. R., and Santos, M. B. L., 1992, *Meas. Sci. Technol.*, **3,** 643.
[19] Tritton, D. J., 1988, *Physical Fluid Dynamics*, 2nd. Edn (Oxford, New York).
[20] Dubois-Violette, E., Guyon, E., and Pieranski, P., 1974, *Mol. Cryst. liq. Cryst.*, **26,** 193.
[21] Jayalakshmi, Y., and Beysens, D., 1995, *J. Phys. II (Paris)*, **5,** 1067.